IBRACON Structures and Materials Journal
Revista IBRACON de Estruturas e Materiais

ORIGINAL ARTICLE

Temperature field of composite steel and concrete slabs in fire situation

Campo térmico de lajes mistas em situação de incêndio

Fabrício Longhi Bolina[a] (ID)

João Paulo Correia Rodrigues[b] (ID)

aUniversidade do Vale do Rio dos Sinos – Unisinos, Escola Politécnica, São Leopoldo, RS, Brasil

bUniversidade de Coimbra, Civil Engineering Research and Innovation for Sustainability – CERIS, Departamento de Engenharia Civil, Coimbra, Portugal

Abstract: Composite steel decking concrete slabs are an important structural member in building construction. Research on its thermal behavior should be developed to understand its fire performance. In this paper, a comparison of the temperature distribution in the cross-section of steel decking concrete slabs subjected to fire is made through three different procedures: (a) standardized analytical, (b) experimental and (c) numerical. The analytical method was the one proposed in NBR 14323 standard. The experimental tests corresponding to eight real-scale fire tests on composite slabs carried out by the authors. The numerical tests were done for the same configurations of the experimental tests and used the FEA software Abaqus. Steel decking temperatures obtained with NBR 14323 methodologies showed good convergence with the experimental and numerical ones. The same was not observed for the concrete, positive and negative rebar.

Keywords: fire, steel decking, concrete; composite slab, thermal behavior, experimental, numerical, analytical.

Resumo: As lajes mistas de aço e concreto (steel deck) trata-se de um importante elemento construtivo de edifícios estruturados. Pesquisas sobre o seu comportamento em altas temperaturas devem ser conduzidas para compreender o seu desempenho ao incêndio. Neste estudo, comparou-se a distribuição de temperatura na seção transversal (isotermas) destas lajes através de três procedimentos: (a) analítico, (b) experimental e (c) numérico. O procedimento analítico é o proposto pela norma NBR 14323. Os testes experimentais correspondem a oito protótipos de lajes ensaiados em escala real pelos autores. A parte numérica foi feita com a mesma configuração da experimental usando o método dos elementos finitos com o software Abaqus. No caso das temperaturas médias da chapa do deck metálico, notou-se convergência entre as obtidas pelo procedimento analítico da NBR 14323 e os resultados experimentais e numéricos. O mesmo não ocorreu para as isotermas do concreto, bem como armaduras positivas e negativas.

Palavras-chave: incêndio, concreto, lajes mistas de aço e concreto, comportamento térmico, experimental, numérico, analítico.

1. INTRODUCTION

Fire is one of the most severe events to which a structure can be subjected during its life. In composite steel and concrete structures, as both structural materials are responsible for the mechanical resistance, they should ensure the structural integrity of the element in case of fire. In these slabs, the profiled steel decking acts as a continuous positive reinforcement and eliminate the need of formwork and steel rebars [1], [2]. When these slabs are subjected to fire on their bottom surface, the steel of the decking degrades leading the slab to behave

as non-reinforced. It is necessary to experimentally study the structural response of these slabs in fire [3]–[4]. The results of some tests [5] have allowed the development of analytical procedures such as the ones presented at EN 1994-1.2 [3]. These methods were the bases of other international standards for fire design of composite structures such as the ANSI/AISC 360-05 [6], BS 5950-8 [7], AS/NZS 2327 [8], NBR 14323 [9].

NBR 14323 has simplified analytical procedures and reference tables for determining the fire resistance of these slabs based on the temperature distribution. These are procedures for assessing temperatures on the decking, concrete and rebars. Since temperature distribution is an important factor in this procedure in fire design, it must be thoroughly investigated [10].

There are a few experimental studies on the temperature distribution in composite slabs [11]. Most of the experimental and numerical research have been conducted for assessing the mechanical behavior, analyzing parameters such as the concrete strength [12], mechanical loading [13], concrete-steel decking longitudinal shear [14], slab-beam interaction [15], steel decking geometry [16] and use of additional steel reinforcement [17], in case of fire. These studies are based on simplified calculation procedures of the cross-section temperature without experimental validation [18], [19]. Thus, more experimental studies are necessary for developing new methods of assessing the temperature distribution in the cross-sections of steel decking concrete slabs [11].

The major part of the numerical simulations of composite steel and concrete elements has used up to now standard thermal parameters. However, some standard parameters seem to be obsolete [20] because they do not encompass all thermophysical mechanisms affected by the temperature. Some authors state that these thermal parameters are unrealistic [21], [22] because they are obtained in small scale tests [23]. They stress the need to find new thermal parameters on full scale tests [24]. Additionally, design criteria for composite slabs subjected to fire have not been revised for decades [20] and sorely need to be updated.

In this sense, different authors [2], [11], [21] have found discrepancies between the experimental and EN 1994-1.2 thermal parameters for materials. These discrepancies extended down to elementary parameters such as the concrete thermal diffusivity and conduction. In some cases, the temperatures in the slab surface, not directly exposed to fire, did not exceed 100°C. As this temperature was related to the thermal diffusivity and temperature distribution in the cross-section, the authors concluded that the standard parameters are oversimplified and far away from the reality [25]. It is known that standard parameters are excessively conservative, when comparing experimental with numerical and analytical results [26].

Experimental research where was calibrated the temperature distribution in the cross-section of composite steel and concrete slabs in fire, was carried out by Usmani et al. in 2001 [27]. However, these authors removed the steel deck before fire test, as they understood that it could be neglected due to its small mechanical contribution at high temperatures. On the other hand, it is currently known that the steel deck interferes in the temperature distribution in the cross-section of the composite slab, due to its emissivity and shadow effect [11]. Nonetheless, the results of this study were considered important because new thermal conductivity parameters were obtained [27]. Others thermal properties have been tested by Kodur [24], in 2014, Al-Sibahy and Edwards [28], in 2012 and Othuman and Wang [29], in 2011.

The simplified calculation methods presented in Annex D of EN 1994-1-2 [1] were obtained from numerical models calibrated with experimental results extracted from Both [5], in 1998. However, there is a standard inconsistency at EN 1994-1-2 because the thermal parameters used on its simplified calculation method of Annex D are different the ones recommended for numerical modeling. This shows the need of uniform and review of these standard thermal parameters. The Brazilian Standard NBR 14323 use the same procedure of EN 1994-1-2.

This paper analyses the distribution of temperatures on the cross-section of steel decking concrete slabs in fire. They are compared experimental with numerical and analytical results. The numerical model was calibrated with results of fire resistance tests carried out by the author. These results were after compared with those calculated with the procedure of the simplified calculation method of NBR 14323 [9]. The comparisons were done for different parts of the slabs: decking, concrete, positive and negative rebars and thermal insulation.

2. METHODS

The description of these procedures is detailed below.

2.1 Slabs characteristics

Figure 1 shows the cross-section of the steel decking concrete slab tested in this research. For temperature measurements, two alignments have been considered. Section A, that is the alignment corresponding to the top flange of the decking and section B corresponding to the bottom flange alignment.

Cross-section of Figure 1 was used to compare the standard, numerical and experimental temperatures of the (i) steel decking, (ii) concrete, (iii) positive and (iv) negative rebars..
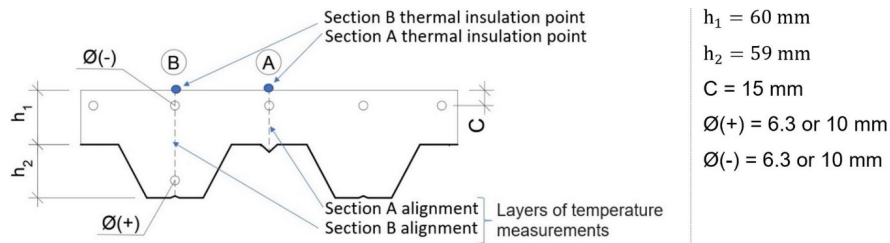

Figure 1 – Cross-section for the standard, numerical and experimental temperature analysis: positive and negative rebars, concrete and steel decking

2.2 Experimental fire tests

This section describes the experimental research procedures. For more information, see the research carried out by the author in [30]–[31].

2.2.1 Materials

The cement used was a high-initial resistance type that contained fewer chemical cement additions. It is a Portland cement used in Brazil, classified as CP-V ARI by NBR 16697 [32]]. No additional chemical additives were incorporated. The gravel used was a dacite with plagioclase and quartz based, and had maximum dimensions of 9.5 mm and 19 mm. A natural quartz and an industrialized dacite sand were used.

The concrete mix was 1:0.91:0.73:0.73:2.18:0.45 (cement: 9.5 mm gravel: 19mm gravel: industrialized sand: natural sand: water) and is shown in Table 1.

Table 1 – Concrete mix used in the specimens

Material	Non-normalized mixing ratio (kg/m³)	Mixing ratio
Portland cement	440	1.00
9.5 mm gravel	400	0.91
19 mm gravel	320	0.73
Industrial sand	320	0.73
Natural sand	960	2.18
Water	200 ± 20	0.45 ± 0.05

The average compression strength of the concrete at 28 and 540 days were 39.6 MPa and 42.4 MPa, respectively. The compression strength of the concrete was determined in accordance with ASTM C39 [33].

Reinforcements had a tensile strength of $f_y = 500$ MPa, classified as CA50 according to NBR 7480 [34]. The rebar diameters were 6.3 mm and 10 mm. The concrete cover of the steel reinforcement was 15 mm in all cases (positive and negative rebars).

The profiled steel decking had 0.80 mm thick, 59.0 mm profile height and cross-sectional area of 1 137.64 mm²/m. The steel used was an ASTM A653 with a tensile strength of f_y=280MPa. The steel decking had a weight of 9.14 kg/m² and an effective width of 915 mm.

In addition, the reduction factors of the mechanical resistance of the concrete and steel in function of the temperature were determined according to ASTM C39 [33] and DIN ISO 6892-2 [35] procedures (Table 2).

Table 2 – Reduction factors for the mechanical resistance of the steel and concrete

Material		Temperature (°C)									
		20	100	200	300	400	500	600	700	800	900
Steel deck	$f_{yk,\theta}/f_{yk}$	1.00	0.94	0.86	0.71	0.60	0.43	0.32	-	-	-
Concrete	$f_{c,\theta}/f_{ck}$	1.00	1.00	1.00	0.95	0.85	0.65	0.31	0.28	0.21	0.10

2.2.2 Slabs prototype and experimental set-up

Table 3 presents the cross-sections of the slabs tested. The differences between the S1-S8 slabs are the diameter of positive and negative rebars. Slabs S6 up to S8 were identical and used as reference. The serviceability load on the slabs were 1.60 kN/m².

Table 3 – Characteristics of the steel decking slabs (experimental specimens)

Specimen	Positive rebars diameter (mm)	Negative rebars diameter (mm)	Cross-section
S1	No positive rebars	No negative rebars	
S2	Ø6.3	No negative rebars	
S3	Ø10	No negative rebars	
S4	No positive rebars	Ø6.3	
S5	No positive rebars	Ø10.0	
S6	Ø6.3	Ø6.3	
S7	Ø6.3	Ø6.3	
S8	Ø6.3	Ø6.3	

Figure 2a presents the test assembly while Figure 2b shows structural design of S6 to S8 slabs, which are similar to all other slabs (i.e., S1-S5).

An auxiliary concrete frame with an intermediate beam (fire protected) was used to create two slab panels of 230 cm each (Figure 3a). This intermediate beam induced negative moments in the slab (stresses in the negative rebars). The experimental model tried to reproduce a real situation of a two-panel slab. All slabs were tested with 540 days of age. The specimen ready for the testing are shown in Figure 3b. Figure 4 shows a view of the horizontal furnace with the eight gas burners working. The heating curve followed the ISO 834 standard fire curve [4].
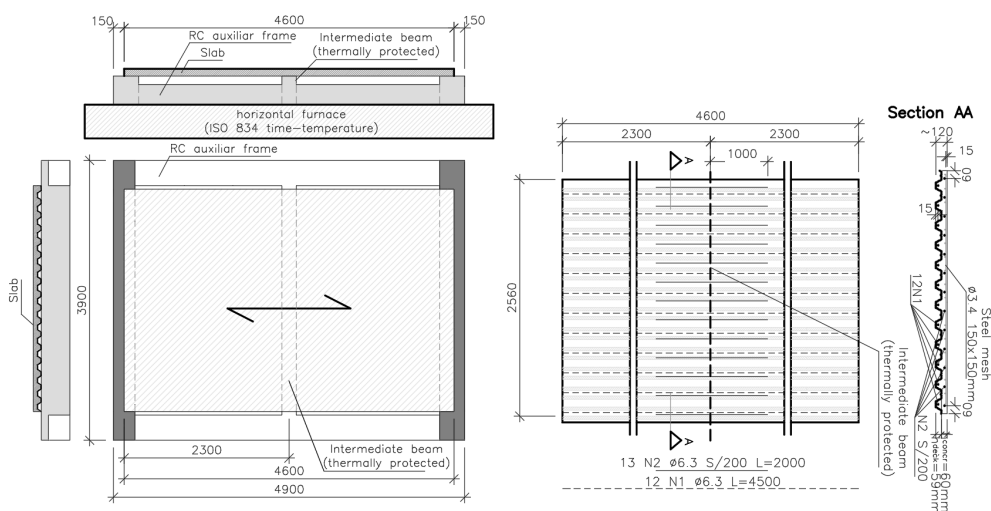

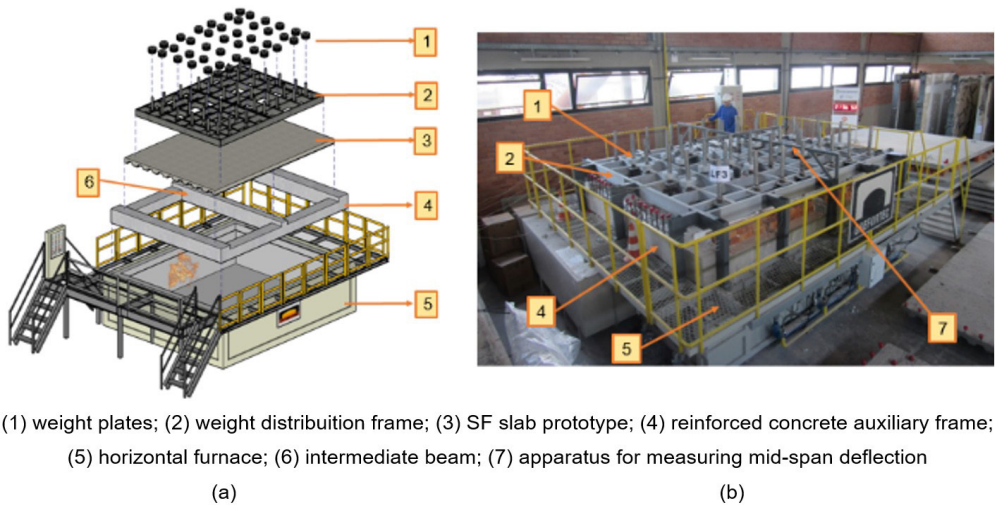**Figure 2 –** (a) Testing assembly and (b) structural drawings of the slabs

Rev. IBRACON Estrut. Mater., vol. 17, no. 2, e17208, 2024

4/17

(1) weight plates; (2) weight distribuition frame; (3) SF slab prototype; (4) reinforced concrete auxiliary frame;
(5) horizontal furnace; (6) intermediate beam; (7) apparatus for measuring mid-span deflection

(a)   (b)

Figure 3 – (a) experimental set-up and (b) procedures (SF prototypes)
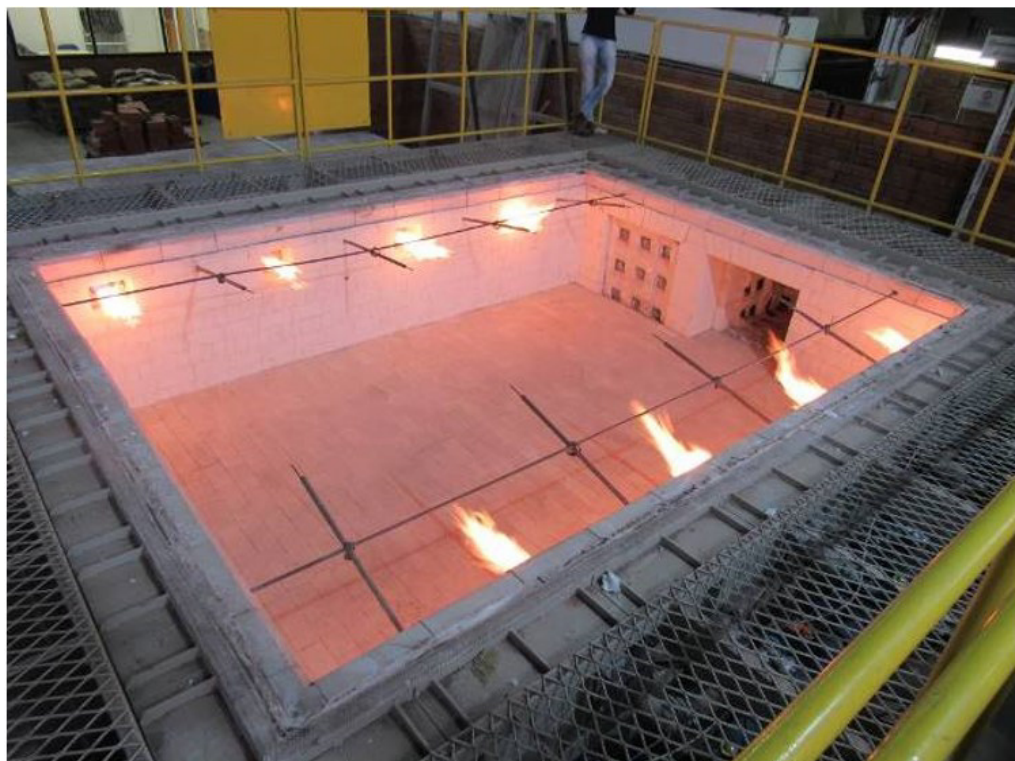
Figure 4 – Horizontal furnace

The experimental tests were carried out according to BS EN 13381 [36].

The history of the internal heating temperatures of the horizontal furnace was carried out using a thermocouple. The temperature sensors (thermocouples) inside the horizontal furnace were K-type with 6.0 mm diameter. A total of 6 thermocouples were used inside the furnace to control the exposure temperatures of the slabs (i.e., temperature applied to their bottom surface). They were placed in the internal environment of the furnace to control the test temperatures. Readings were continuously recorded from a data acquisition system that is part of the furnace.

2.2.3 Slab prototype temperatures

The specimen's temperatures were measured at sections A and B (Figure 5a). Along the cross-section, the thermocouples were installed at specific intervals (concrete layers): 3 sensors for section A alignment (named 2.5A, 5A and 6A, located at 2.5, 5 and 6 cm from the top surface) and 5 sensors for section B alignment (named 2.5B, 5B, 6B, 8B and 11B, located at 2.5, 5, 6, 8 and 11 cm from the top surface) (Figure 5b). For steel reinforcements, a total of 2 sensors for each (positive/negative) were used. The reinforcements, steel decking and concrete layer temperatures were defined as the average temperature (measured between all the slabs).

Thermocouples named "T" were used to measure the thermal insulation of the slab during the fire test (Figure 5c). Thermocouples T were installed in the slab surface not exposed to fire (sections A of the slab, that is the thinnest part of the slab cross-section, as shown in Figure 1). In panel 1, five thermocouples (T1-T5) were used, while in panel 2, only one thermocouple T6 was placed in the center of that area. The thermal insulation results were taken based from thermocouples T1 to T5 readings. Thermocouple T6 was used only for controlling porpoise.
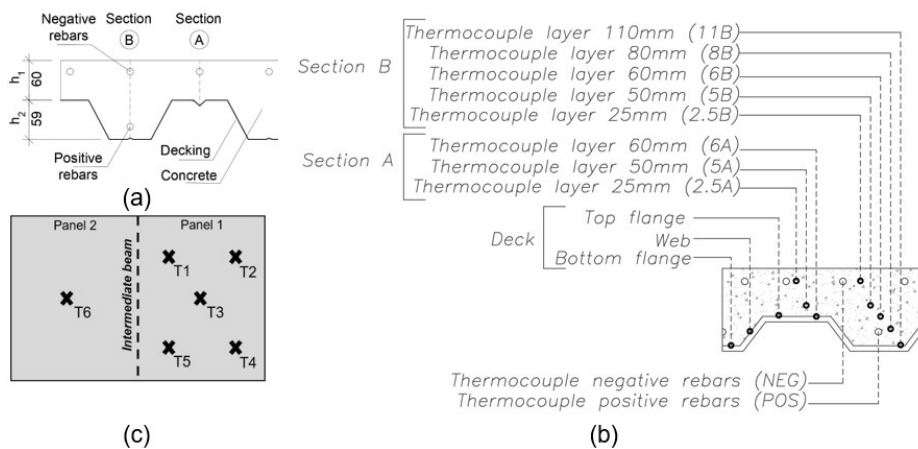

Figure 5 – Slab cross-section: (a) sections A and B and (b) thermocouple location and (c) thermal insulation (slab surface)

2.3 Numerical simulation

The numerical simulations were performed with the FEA Abaqus software [37]. The thermal parameters used in these analyzes, in the different parts of the slab cross-section, are indicated in Figure 6. On the bottom surface of the slab, the ISO 834 fire curve was applied, transmitted by thermal convection (with heat transfer coefficient $\alpha=25$ W/m$^2\times$K) and radiation (with thermal emissivity $\varepsilon=0.40$, as suggested by Jiang et al. [20]). On the top surface of the slab, the ambient temperature was 25ºC, transmitted to the surface by convection (with heat transfer coefficient $\alpha=9$ W/m$^2\times$K).

The profiled steel decking detached from the concrete in the initial stages of the fire exposure (Figure 7), as noted in the experimental test. This air layer directly affected the isotherms in the slab cross-section and was incorporated in the FEA-model, with a thickness of 15mm. The thicknesses of the air layer assumed in the numerical analysis is that identified by visual perceptions in the experimental tests (see Figure 7). The concrete cover assumed in the FEA-numerical procedures was the same used experimentally, as shown in Figure 1. The location of the reinforcements in the cross section of the slab was the same adopted in the laboratory prototypes, using the same criteria shown in Figure 2.
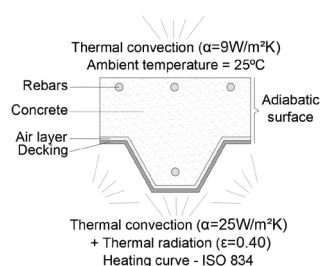

Figure 6 – Cross-section thermal parameters

Rev. IBRACON Estrut. Mater., vol. 17, no. 2, e17208, 2024

6/17

Figure 7 – Detachment of the steel decking during test

The steel decking was modeled with a 4-node shell element (S4RS), the reinforcement with a beam of 2-node link (B31) and the concrete with a general 3D solid 8-node brick element with reduced integration (C3D8R) from Abaqus library. A mesh analysis was performed and the mesh was rather refined, the size of the elements was 0.5 x 0.5 mm for S4RS, 0.5 mm for B31 and 0.5 x 0.5 x 0.5 mm for C3D8R. This refined mesh was necessary mainly due to the problem of the interface between the concrete and the decking, and also due to the geometry of the steel decking. This mesh showed better convergence with the obtained experimental results (used for FEA-model validation).

The values of the thermal conductivity and specific weight variation of the concrete with the temperature were extracted from NBR 14323 [9]. The thermal conductivity and specific heat of the steel rebars were taken from NBR 14323 [9]. Rebars and steel decking were considered with a density of 7850 kg/m^3. The thermal conductivity of the steel of the steel decking was taken from Craveiro et al. [1]. The specific heat of conventional steel structures of NBR 14323 [9] was used in the decking. Air thermal properties (specific heat, thermal conductivity and specific weight) were considered according the Çengel and Ghajar [38] criterion.

The FE-model used to the decking was a two-layer shell (composite layup in Abaqus): one layer with the thermal properties of the steel (with the respective thickness of the decking) and another layer with the thermal characteristics of the air (and their respective thickness). In Abaqus software, "conventional composite shell layouts" are used in composite layers made from different materials in different orientations.

In the numerical model, an effective heat flux (h_{net}) was determined based on the convective ($h_{net,c}$) and radiative ($h_{net,r}$) heat fluxes. Other constants were defined, as the absolute zero temperature (-273.15 ºC), Stefan-Boltzmann constant (σ=5.67 x 10^{-8} W/m^2.K^4), gas temperature (θ_g, obtained from the ISO 834), initial surface temperature (θ_m = 25 ºC) and initial radiation temperature of the surface (θ_r = 25 ºC), configuration factor (ϕ = 1.0), convection heat transfer coefficient (α_c= 25 W/m^{2}K), steel decking surface emissivity (ε_m = 0.40) and fire emissivity (ε_f = 1.00).

2.4 Analytical procedures

This section describes the method used in the analytical procedure. It was used the simplified method of annex D of EN 1994-1.2 [3] and C of NBR 14323 [9] standards.

2.4.1 Temperature in the concrete

The temperature in the concrete was calculated according to item D.3 of EN 1994-1.2 [3] and item C.2 of NBR 14323 [9]. The standard procedures defined a critical isotherm temperature defined by four coordinates X_I, X_{II}, X_{III}, X_{IV} and Y_I, Y_{II}, Y_{III}, Y_{IV} in the slab cross-section, respectively. Portions of the slab above the critical isotherm were considered not affected by temperatures. The critical temperature is given by Equation 1. This is a standardized procedure used to define the critical temperature (i.e., isotherm) for the fire-design the hogging bending moment of these slabs.

$$\theta_{lim} = d_0 + d_1 \times N_s + d_2 \times \frac{A}{L_r} + d_3 \times \Phi + d_4 \times \frac{1}{l_3} \; [°C] \tag{1}$$

where the factors are described in EN 1994-1.2 [3] and NBR 14323 [9].

2.4.2 Temperature of the profiled steel decking

The analytical steel decking temperature was calculated according to item D.2 of EN 1994-1-2 [3] and C.2 of NBR 14323 [9] as shown in Equation 2:

$$\theta_i = b_0 + b_1 \times \frac{1}{b_2} + b_2 \times \frac{A}{L_r} + b_3 \times Ø + b_4 \times Ø^2 \ \ [°C] \tag{2}$$

where b_0, b_1, b_2, b_3 and b_4 are tabulated coefficients defined for 60, 90 and 120 min of the ISO 834 [4]. The parameter Φ is a configuration factor of the top flange of the profiled steel decking calculated with the Hottel and Cohen's law [39].

2.4.3 Temperature of the tension (positive) rebars

The temperature of the positive rebars was calculated according to Annex D of EN 1994-1-2 [3] and annex C of NBR 14323 [9] as shown in Equation 3.

$$\theta_s = c_0 + c_1 \times \left(\frac{u_{f3}}{h_f}\right) + c_2 \times z + c_3 \times \frac{A}{L_r} + c_4 \times \alpha + c_5 \times \frac{1}{b_2} \ \ [°C] \tag{3}$$

where z is relative to the rebar position in the cross-section, u_1, u_2 and u_3 are the shortest geometric distances from the rebar axis to the steel decking and c_0, c_1, c_2, c_3, c_4 and c_5 are coefficients defined in EN1994-1.2 [3] and NBR 14323 [9] standards.

2.4.4 Temperature of the compression (negative) rebars

Section D.3 of the EN 1994-1-2 [3] and C.2 C of NBR 14323 [9] supposes that the negative reinforcements are at ambient temperature. The logic behind this is that, based on the critical temperature, depending on the isotherm coordinates X_n and Y_n, portions of the slab above the isotherm (which include the negative reinforcement) could be assumed to be unaffected by the temperature. In this research, the critical temperature was limited to 500°C in accordance to FIB Bulletin nº 38 [40].

3 RESULTS

In this section they are first presented the calibration of the numerical models with the experimental results. Then, the experimental and numerical results were compared with those obtained by NBR 14323 [9] analytical methods (simplified method).

3.1 Comparison between Experimental and Numerical Temperatures (validation)

This section aims to validate the numerical model based on the experimental results.

Figure 8 shows the evolution of the furnace temperatures in all experimental tests (i.e., experimental specimens shown in Table 3) comparing with the ISO 834 fire curve limits. These curves show the reproducibility of the experimental test results.
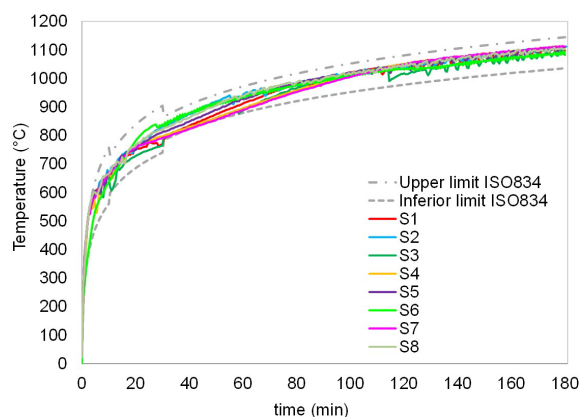

Figure 8 – Furnace temperatures in all experimental tests and ISO 834 fire curve

Rev. IBRACON Estrut. Mater., vol. 17, no. 2, e17208, 2024

8/17

Figure 9 presents the isotherms in the slab's cross-section for 30, 60, 90, 120, 150 and 180 min of exposure to the ISO 834 fire curve. There is a non-uniform temperature distribution in the slab cross-section, having the thinnest part of the slab (section A) higher temperatures than the thickest part (section B).
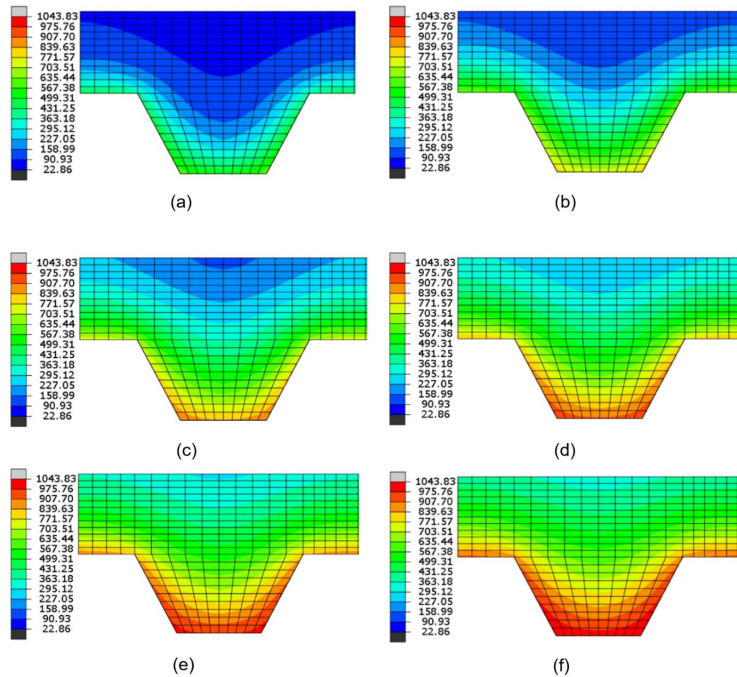

(a)   (b)

(c)   (d)

(e)   (f)

Figure 9 – Isotherms for h_1 = (a) 30; (b) 60; (c) 90, (d) 120, (e) 150 and (f) 180 min of exposure to the ISO 834 fire curve (temperatures in ºC).

Figure 10 shows the temperatures' distribution in section A, while Figure 11 in section B. Figure 12 shows the temperatures of the positive and negative rebars in sections A and B. Fig. 13 shows the temperatures in the unexposed slab surface (thermal insulation). The values in Figures 10 to 13 were used to validate the thermal parameters and numerical model. These thermal fields resulted from the slab's heating according to the ISO 834 fire curve. The temperatures of the experimental results (in the respective layer) refer to the average of the temperatures obtained in the 8 prototypes of composite slabs tested experimentally (see Table 3). The experimental temperatures (named as "exp") were those measured by thermocouples (see Section 2.2.3) and those of the numerical model (named as "num") by temperature controllers inserted in the FEA-simulation (at the same points assumed in the experimental model, i.e., according to Figure 5b).
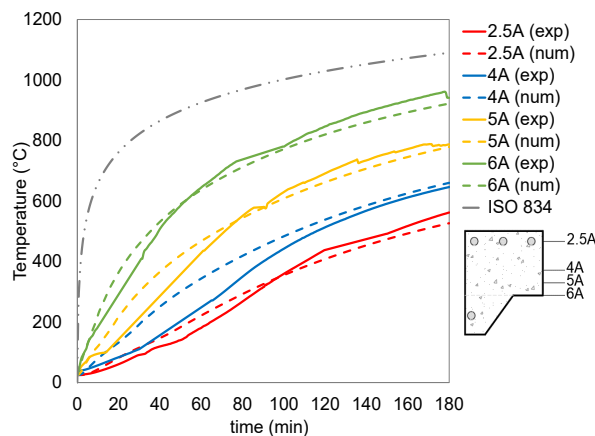

Figure 10 – Numerical and experimental temperatures for section A of the slabs
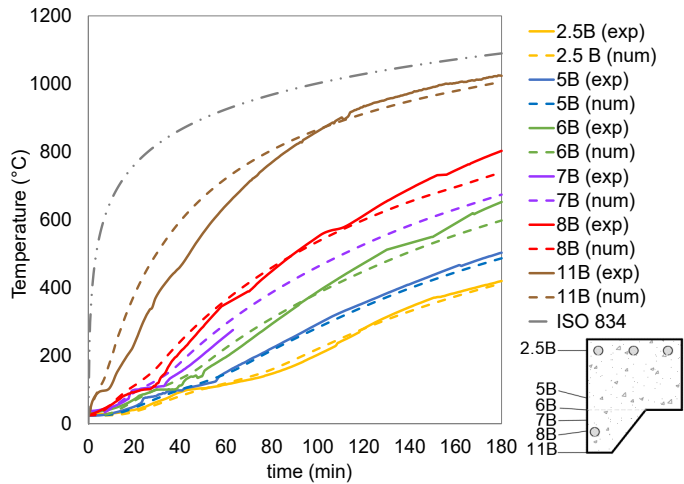
Figure 11 – Numerical and experimental temperatures for section B of the slabs
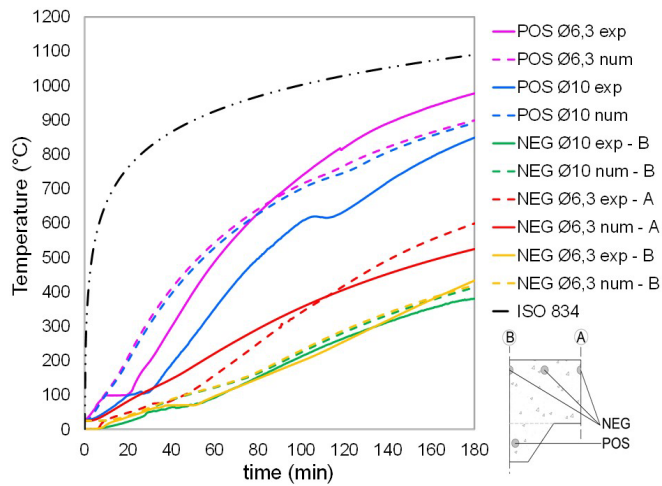

Figure 12 – Numerical and experimental temperatures for positive and negative rebars of the slabs
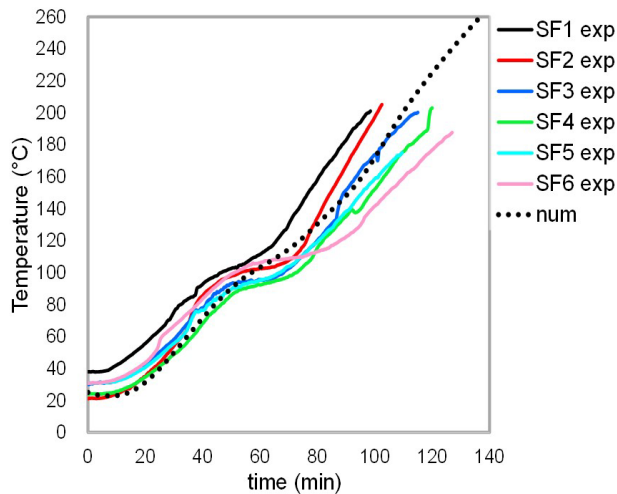

Figure 13 – Numerical and experimental temperatures for thermal insulation in section A of the slabs

Rev. IBRACON Estrut. Mater., vol. 17, no. 2, e17208, 2024

10/17

Figures 10 and 11 show that the temperatures of the steel decking (6A for section A and 11B for section B) were lower than the ISO 834 [4] fire curve ones. This fact mainly results from the steel decking emissivity and the sink effect of the slab. Figures 10 and 11 also show that, at the same cross-section depths, the temperatures in section A were always higher than the ones in section B, due to its smaller thickness (also according to Figure 9 results). The small differences between the experimental and numerical are from the variability of the experimental results. In the experimental tests may occur, e.g., concrete cracking, mass and heat transfer and chemical changes, that are not considered in the numerical simulations. Figure 11 also shows the temperature in the concrete layer close to the reinforcement (points 8B for positive and 2.5B for negative reinforcement). Note that the concrete temperature in these layers is similar to the respective temperature in the rebars positioned in the region. The temperatures in these reinforcements are shown in Figure 12.

Figure 12 shows that the negative rebars were more thermally protected than the positive ones, with temperature's difference reaching 300°C. The position of the negative rebars in the cross-section (section A or B) influences their temperature. The variation between the temperatures of the positive rebars with diameters from Ø6.3 to Ø 10 mm, is small. There is a sensitive difference between the experimental and numerical results. This is due to the difficulty of exact positioning of the reinforcement in the construction of the experimental specimens, as well as the concrete cracking during the experimental tests, which can alter the laboratory results in relation to the FEA-numerical models. Figure 13 shows the convergence of the thermal insulation results between SF1-SF6 slabs and the numerical model.

Figures 10 to 13 also show that there was an agreement between the experimental and numerical temperature results and thus the EN 1994-1.2 [3] and NBR 14323 [9] thermal parameters of the materials were adequate for numerical modelling of this type of slabs.

The research [5] that gave rise to the simplified method of NBR 14323 [9] and EN 1994-1.2 [3] did not use the material parameters that are actually indicated in the Eurocode, which is contradictory. It is recommended that Both [5] criterion is used, but with the parameters currently used by the standard. Alternatively, there is an analytical method that was proposed by Bolina and Rodrigues [30] that can be used as a reference.

3.2 Comparison: NBR 14323, Experimental and Numerical Temperatures

3.2.1 Temperatures of the profiled steel decking

Figures 14 to 16 present a comparison of the profiled steel decking temperatures calculated with the NBR 14323 [9] and EN1994-1.2 [3] and the experimentally and numerically determined ones for 60, 90 and 120 min of the ISO 834 [4] fire curve. Figure 17 shows the temperatures of the web, bottom and top flanges defined by FEA-numerical models, and also their average temperature developed during the exposure of the ISO 834 fire curve (numerical results).
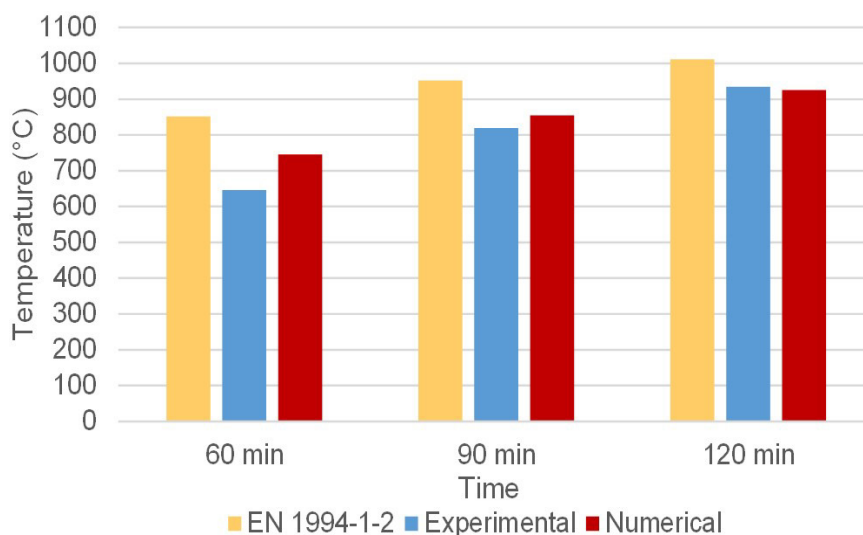

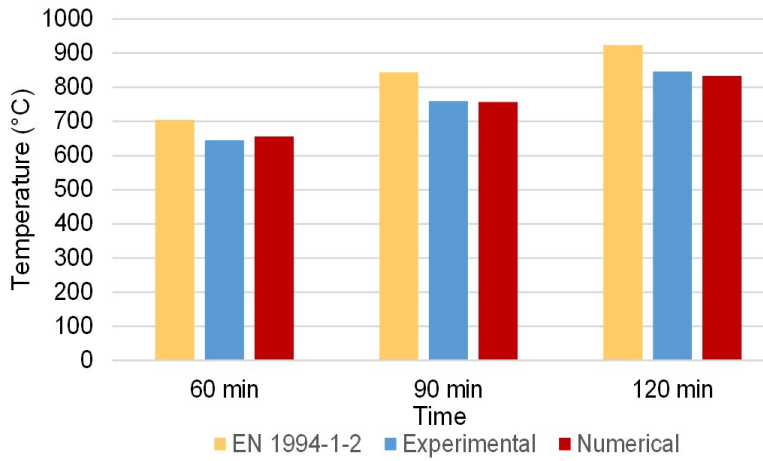**Figure 14** – Temperatures in the bottom flange of the steel decking

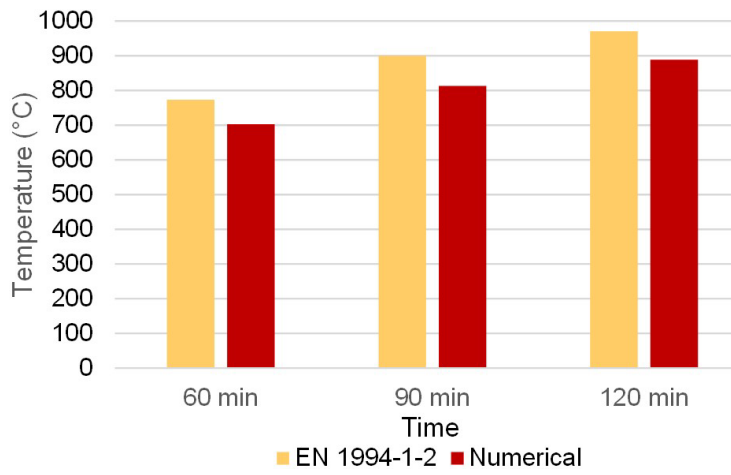**Figure 15** – Temperatures in the top flange of the steel decking

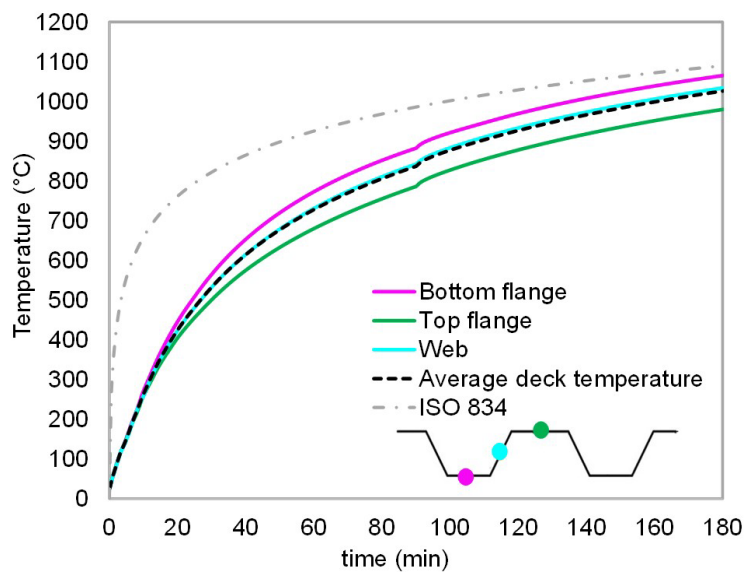**Figure 16** – Temperatures in the web of the steel decking

Figure 17 – Temperatures in the web of the steel decking

Rev. IBRACON Estrut. Mater., vol. 17, no. 2, e17208, 2024

12/17

The results show that both the experimental and numerical temperatures are lower than the ones determined with the procedures of the simplified calculation method of NBR 14323 [9] and EN 1994-1-2 [4].

Comparing the analytical and numerical temperatures, the largest difference occurred in the bottom flange, where the analytical was 14.2% higher than the numerical. The maximum difference between the experimental and numerical temperatures was 8%, at 60 min, while the minimum was 1.3%, at 120 min. This agreement validated the EN 1994-1-2 [4], NBR 14323 [9] and Craveiro et al. [1] thermal parameters for numerical modeling of these elements. The steel decking temperatures practiced in the NBR 14323 [9] analytical method was higher than the numerical and experimental ones, showing the conservatism of the standard procedures. The temperatures numerically and experimentally obtained were on average 100ºC lower than the standard ones.

3.2.2 Temperatures of concrete

EN 1994-1.2 [3] and NBR 14323 [9] allow to determine the coordinates of the temperature limit isotherm. The temperatures in the concrete were not uniform along the cross-section. In almost all cases of Table 4, the temperatures of the numerical model, for the same coordinates, were higher than the EN 1994-1-2 and NBR 14323 ones. However, with the time increasing, the difference decreased to the point that the average numerical temperatures were lower than the analytical ones, at 120 min. In qualitative terms, the numerical temperatures were 15.9% higher at 60 min, 2.6% higher at 90 min, and 2.3% lower at 120 min, than the analytical ones.

Table 4 – Comparison between EN1994-1.2 and numerical temperatures

Time (min)		Temperature (°C)				
		Numerical simulations				
	Standard	Coordinates				
		X_I, Y_I	X_{II}, Y_{II}	X_{III}, Y_{III}	X_{IV}, Y_{IV}	Average
60 (I)	510.6	626.0	662.3	510.0	569.8	592.0
90 (II)	635.3	697.7	735.0	575.0	600.8	652.1
120 (III)	719.0	764.7	785.4	633.2	627.0	702.6

The origin of the standardized analytical method was based on Both's numerical and experimental studies [5]. In his numerical research, the author used concrete thermal parameters different from those currently recommended by the standard. Therefore, there is a divergence between criteria: the standard's analytical method was designed with parametric data different from what it currently recommends.

3.2.3 Temperatures of positive reinforcements

Experimental and numerical positive rebar temperatures are compared to the analytical ones calculated with NBR 14323 [9] procedures.

Figures 18 and 19 show that analytical temperatures defined with NBR 14323 [9] and EN 1994-1.2 [3] procedures were always higher than both the experimental and numerical ones. This was similar to what occurred in the steel decking but different with the concrete. In the 6.3 mm rebars, analytical temperatures were more than 40% higher than the experimental ones. In the case of 10 mm rebars, analytical temperatures were more than 29.9% higher than experimental ones. Comparing the analytical with the numerical temperatures, the maximum difference was 26.1% higher.
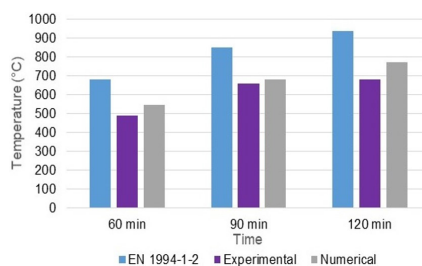

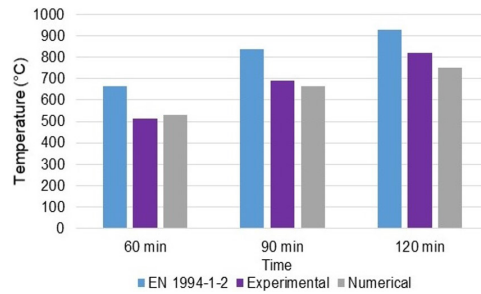**Figure 18** – Comparison of Ø6.3 mm positive rebar

Figure 19 – Comparison of Ø10 mm positive rebar

In the case of the positive reinforcements the differences between the analytical, experimental and numerical temperatures results are justified by the origin of the analytical method of EN 1994-1.2 [3] and NBR 14323 [9] standards. The analytical method is the result of research carried out by Both [5]. This research was carried out with thermal parameters for concrete and steel different from those currently indicated in the standards. This means that composite steel and concrete slabs numerically calculated with the standardized thermal parameters may present temperatures different from those calculated with the standardized analytical method.

3.2.4 Temperatures of negative reinforcements

EN 1994-1.2 [3] and NBR 14323 [9] does not provide a methodology for assessing the temperatures of the negative rebars. In Figures 20 to 23 are presented the results of the numerical temperatures in function to the ISO 834 with h1 of 40, 50, 60 and 70 mm, respectively, all with h2= 59 mm. For each case, it was used concrete rebar covers (C) of 10, 20 and 30 mm.
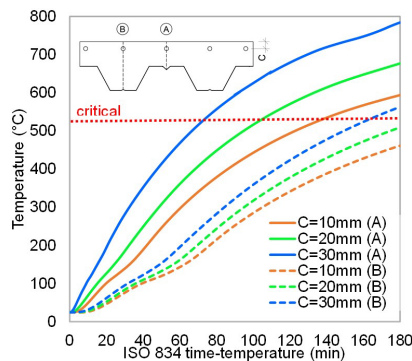

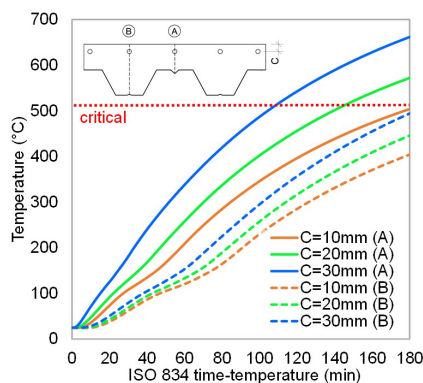**Figure 20** – Temperatures of the negative rebars for h_1= 40 mm and h_2= 59 mm

Figure 21 – Temperature of negative rebars for h_1= 50 mm and h_2= 59 mm
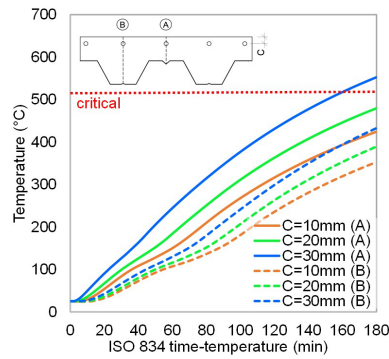
Figure 22 – Temperatures of negative rebars for h_1= 60 mm and h_2= 59 mm
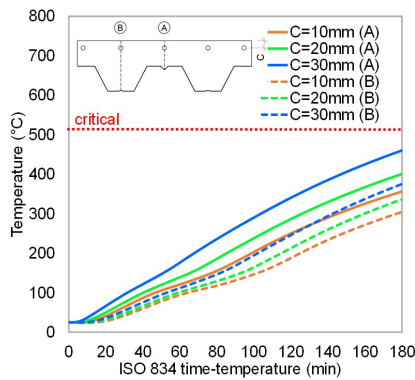

Figure 23 – Temperatures of negative rebars for h_1= 70 mm and h_2= 59 mm

Figures 20 to 23 shows that the temperatures of the negative rebars are affected by their position in the slab cross-section. Rebars placed above the top flange (section A) showed higher temperatures than those placed above the bottom flange (section B) of the steel decking. This temperature difference between the rebars positioned in section A and B was in the order of 300 °C. It should be noted that this aspect of the negative rebar location within the slab is not foreseen in EN 1994-1.2 [3] and NBR 14323 [9] procedures.

4 CONCLUSIONS

The general conclusions of this paper are:
- The steel decking detachment occurred very early in the fire resistance tests (initial 5 minutes of exposure to the ISO 834 fire curve). This suggested that the composite slab did not behave as a composite structure when in fire situation;
- The detachment of the steel decking was not influenced by the arrangement and amount of added supplementary reinforcements. This detachment depends on the temperature of the steel decking (thermal-physical effects) and its interaction with the concrete;
- Steel decking temperatures determined analytically by EN 1994-1-2 and NBR 14323 showed convergence with the experimental and numerical ones;
- Positive rebar temperatures analytically calculated with the EN 1994-1-2 and NBR 14323 procedures were higher than the experimental and numerical ones. This is possibly justified by the origin of this standard method, which was extracted from Both [5], that admitted thermal parameters for the concrete and steel different from what is currently practiced in the Eurocode;
- Negative rebar temperatures were mostly not affected by fire conditions, but there are cases when its heating cannot be neglected. NBR 14323 and EN 1994-1-2 are in need of a revision;
- The authors suggest that a new research should be developed to evaluate the influence of the temperature difference between standard and experimental/numerical procedures on the mechanical performance of the composite slab in fire.

REFERENCES

[1]   H. D. Craveiro, J. P. C. Rodrigues, A. Santiago, and L. Laim, "Review of the high temperature mechanical and thermal properties of the steels used in cold formed steel structures - The case of the S280GD+Z steel," *Thin-walled Struct.*, no. 98, pp. 154–168, 2016, http://dx.doi.org/10.1016/j.tws.2015.06.002.

[2]   D. Pantousa and E. Mistakidis, "Advanced modeling of composite slabs with thin-walled steel sheeting submitted to fire," *Fire Technol.*, vol. 49, no. 2, pp. 293–327, 2013, http://dx.doi.org/10.1007/s10694-012-0265-x.

[3]   European Committee for Standard, *Design of Composite Steel and Concrete Structures. Part 1.2 - Design Rules, Structural Fire Design,* EN 1994-1-2, 2011.

[4]   International Organization for Standardization, *Fire Resistance Tests - Elements of Building Construction,* ISO 834-8, 1999.

[5]   C. Both, "*The fire resistance of composite steel-concrete slabs,*" M.S. thesis, Delft University of Technology, Delft, The Netherlands, 1998.

[6]   American Institute of Steel Construction, *Specification for Structural Steel Building,* ANSI/AISC 360-05, 2005.

[7]   British Standard, *Structural Use of Steelwork in Building, Part 8: Code of Practice for Fire Resistant Design,* BS 5950-8, 2003.

[8]   Australia Standard/New Zealand Standard, *Composite Steel-Concrete Construction for Buildings,* AS/NZS 2327, 2017.

[9]   Brazilian Standard Association, *Structural Fire Design of Steel and Composite Structures for Buildings,* NBR 14323, 2013.

[10] S. Lamont, A. S. Usmani, and D. D. Drysdale, "Heat transfer analysis of the composite slab in the Cardington frame fire tests," *Fire Saf. J.*, vol. 36, no. 8, pp. 815–839, 2001, http://dx.doi.org/10.1016/S0379-7112(01)00041-8.

[11] J. Jiang, J. A. Main, J. M. Weigand, and F. H. Sadek, "Thermal performance of composite slabs with profiled steel decking exposed to fire effects," *Fire Saf. J.*, vol. 95, pp. 25–41, 2018, http://dx.doi.org/10.1016/j.firesaf.2017.10.003.

[12] J. J. Del Coz-Diaz, J. E. Martinez-Martinez, M. Alonso-Martinez, and F. P. A. Rabanal, "Comparative study of Light-Weight and Normal Concrete composite slabs behavior under fire conditions," *Eng. Struct.*, vol. 207, pp. 110196, 2020, http://dx.doi.org/10.1016/j.engstruct.2020.110196.

[13] K. M. A. Hossain, S. Attard, and M. S. Anwar, "Finite element modelling of profiled steel deck composite slab system with engineered cementitious composite under monotonic loading," *Eng. Struct.*, vol. 186, pp. 13–25, 2019, http://dx.doi.org/10.1016/j.engstruct.2019.02.008.

[14] S. Sharma, V. T. Vaddamani, and A. Agarwal, "Insulation effect of the concrete slab-steel deck interface in fire conditions and its influence on the structural fire behavior of composite floor systems," *Fire Saf. J.*, vol. 105, pp. 79–91, 2019, http://dx.doi.org/10.1016/j.firesaf.2019.02.006.

[15] J.-S. Zhu, Y.-G. Wang, J.-B. Yan, and X.-Y. Guo, "Shear behavior of steel-UHPC composite beams in waffle bridge deck," *Compos. Struct.*, vol. 234, pp. 111678, 2020, http://dx.doi.org/10.1016/j.compstruct.2019.111678.

[16] I. Arrayago, E. Real, E. Mirambell, F. Marimon, and M. Ferrer, "Experimental study on ferritic stainless steel trapezoidal decks for composite slabs in construction stage," *Thin-walled Struct.*, vol. 134, pp. 255–267, 2019, http://dx.doi.org/10.1016/j.tws.2018.10.012.

[17] L. G. F. Grossi, C. F. R. Santos, and M. Malite, "Longitudinal shear strength prediction for steel-concrete composite slabs with additional reinforcement bars," *J. Construct. Steel Res.*, vol. 166, pp. 105908, 2020, http://dx.doi.org/10.1016/j.jcsr.2019.105908.

[18] H. Rezaeian, G. C. Clifton, and J. B. P. Lim, "Failure modes for composite steel deck diaphragms subjected to in-plane shear forces – A review," *Eng. Fail. Anal.*, vol. 107, pp. 104199, 2020, http://dx.doi.org/10.1016/j.engfailanal.2019.104199.

[19] T. Gernay and N. E. Khorasani, "Recommendations for performance-based fire design of composite steel buildings using computational analysis," *J. Construct. Steel Res.*, vol. 166, pp. 105906, 2020, http://dx.doi.org/10.1016/j.jcsr.2019.105906.

[20] J. Jiang, A. Pintar, J. M. Weigand, J. A. Main, and F. Sadek, "Improved calculation method for insulation-based fire resistance of composite slabs," *Fire Saf. J.*, vol. 105, pp. 144–153, 2019, http://dx.doi.org/10.1016/j.firesaf.2019.02.013.

[21] M. Achenbach, T. Lahmer, and G. Morgenthal, "Identification of the thermal properties of concrete for the temperature calculation of concrete slabs and columns subjected to a standard fire — Methodology and proposal for simplified formulations," *Fire Saf. J.*, vol. 87, pp. 80–86, 2017, http://dx.doi.org/10.1016/j.firesaf.2016.12.003.

[22] Z. Xing, A. Beaucour, R. Hebert, A. Noumowe, and B. Ledesert, "Influence of the nature of aggregates on the behavior of concrete subjected to elevated temperature," *Cement Concr. Res.*, vol. 41, no. 4, pp. 392–402, 2011, http://dx.doi.org/10.1016/j.cemconres.2011.01.005.

[23] G. Robert, H. Colina, and G. Debicki, "The durability of concrete in fire", in: J. P. Olivier and A. Vichot, Eds., *Concrete durability: scientific bases for formulating durable concrete according to the environment.* São Paulo: IBRACON, 2014, pp. 605.

[24] V. Kodur, "Properties of concrete at elevated temperatures," *ISRN Civ. Eng.*, vol. 20174, pp. 468510, 2014, http://dx.doi.org/10.1155/2014/468510.

[25] G. Li, N. Zhang, and J. Jiang, "Experimental investigation on thermal and mechanical behavior of composite floors exposed to standard fire," *Fire Saf. J.*, vol. 89, pp. 63–76, 2017, http://dx.doi.org/10.1016/j.firesaf.2017.02.009.

[26] L. Lin and C. Wade, *Experimental fire tests of two-way concrete slabs. Fire engineering research report 02/12.* Christchurch: University of Canterbury, 2002.

[27] A. S. Usmani, J. M. Rotter, S. Lamont, A. M. Sanad, and M. Gillie, "Fundamental principles of structural behavior under thermal effects," *Fire Saf. J.*, vol. 36, no. 8, pp. 721–744, 2001, http://dx.doi.org/10.1016/S0379-7112(01)00037-6.

[28] A. Al-Sibahy and R. Edwards, "Thermal behavior of novel lightweight concrete at ambient and elevated temperatures: Experimental, modelling and parametric studies," *Constr. Build. Mater.*, vol. 31, pp. 174–187, 2012, http://dx.doi.org/10.1016/j.conbuildmat.2011.12.096.

[29] M. A. Othuman and Y. C. Wang, "Elevated-temperature thermal properties of lightweight foamed concrete," *Constr. Build. Mater.*, vol. 25, no. 2, pp. 705–716, 2011, http://dx.doi.org/10.1016/j.conbuildmat.2010.07.016.

[30] FL Bolina and JPC Rodrigues, "Numerical study and proposal of new design equations for steel decking concrete slabs subjected to fire," *Engineering Structures*, vol. 253, pp. 113828, 2022, https://doi.org/10.1016/j.engstruct.2021.113828

[31] F. L. Bolina, B. F. Tutikian, and J. P. C. Rodrigues, "Experimental analysis on the structural continuity effect in steel decking concrete slabs subjected to fire," *Eng. Struct.*, vol. 240, pp. 112299, 2021, http://dx.doi.org/10.1016/j.engstruct.2021.112299

[32] Brazilian Standard Association, *Portland Cement – Requirements*, NBR 16697, 2018.

[33] American Society for Testing and Materials, *Standard Test Method for Compressive Strength of Cylindrical Concrete Specimens,* ASTM C39, 2020.

[34] Brazilian Standard Association, *Steel for the Reinforcement of Concrete Structures – Specification,* NBR 7480, 2007.

[35] Deutsches Institut für Normung, *Tensile Testing Part 2: Tensile Testing Method of test at Elevated Temperature,* DIN EN ISO 6892-2, 2018.

[36] British Standard, *Test Methods for Determining the Contribution to the Fire Resistance of Structural Members: Horizontal protective membranes,* BS EN 13381-1, 2014.

[37] Abaqus, *Abaqus analysis user's guide*. Simulia: Abaqus, 2016.

[38] Y. A. Çengel and A. J. Ghajar, *Heat and mass transfer: fundamentals & applications*. New York: McGraw-Hill Education, 2015.

[39] H. C. Hottel and E. S. Cohen, "Radiant heat Exchange in a gas-filled enclosure: allowance for non-uniformity of gas temperature," *AIChE J.*, vol. 4, no. 1, pp. 3–14, 1958, http://dx.doi.org/10.1002/aic.690040103.

[40] Fédération Internationale du Béton, *Fire Design of Concrete Structures - Materials, Structures and Modelling: State-of-art Report,* FIB Bulletin 38, 2007.